CHAPTER 5

MOLECULAR AND DYNAMICAL PROPERTIES OF TWO PERFLUORINATED LIQUID CRYSTALS WITH DIRECT TRANSITION FROM FERROELECTRIC SmC* PHASE TO ISOTROPIC PHASE

Part of the work has been published in Journal of Molecular Liquids., Vol. 182: pp. 95–101, 2013.

5.1 INTRODUCTION

In 1974, Meyer [1] concluded from symmetry argument that chiral molecules in smectic C phase should exhibit ferroelectricity and such phenomenon was indeed discovered soon in a Schiff's base compound DOBAMBC, thus started a new branch of material science, ferroelectric liquid crystals. These materials are only known intrinsic polar fluid materials that possess the ferroelectric, electro-optic, piezoelectric and pyroelectric properties of solid polar dielectrics with the physical flow characteristics of liquids. After the discovery of antiferroelectricity by Fukuda group [2] in MHPOBC it has been shown that between antiferroelectric and para-electric phases three different sub phases (SmC_{α}^{*} SmC_{β}^{*} and SmC_{γ}^{*}) also exist [2-5] and their stability depends strongly on the optical purity of the compounds [6]. Different types of chiral liquid crystal compounds are found to possess one or more of the phases like antiferroelectric SmC_{A}*, ferroelectric SmC* (including its sub- phases) and paraelectric SmA* phases making them attractive from both theoretical and application points of view. Ferroelectric liquid crystals (FLCs) have been studied extensively due to their various interesting basic properties, FLCs are also promising materials for fast switching electro-optical displays with wide viewing angle [7]. However, they are not used much commercially because of difficulties at various levels. Therefore effort is made to design new materials and study various physical properties so as to overcome these difficulties. Because of the small size of a fluoro substituent and high strength of the C–F bond, liquid crystals with fluoro substituents show low birefringence, viscosity, conductivity and high chemical and thermal stability. As a result many liquid crystal compounds with fluoro substituents both in the cores and alkoxy chains were designed and synthesized in both achiral and chiral systems [8-14]. Liquid crystals with fluorinated chains are also very promising as antiferroelectric materials especially as thresholdless ones [14-17]. Phase behavior, physical and electrooptical properties of fluorinated derivatives in many respects are quite different from their hydrogenous analogues which create new possibilities for their applications [16]. For example, protonated organosyloxane compounds exhibit both SmC^{*} and de Vries SmA^{*} phases [18, 19], but Naciri et al [20, 21] reported that analogous fluorinated compound exhibit only de Vries SmA^{*} phase. A terphenyl based ester compound with CH3COO group at the achiral end exhibits SmC^{*} and SmA^{*} phases while analogous compound with CF3COO group shows SmC^{*}_{A} phase in addition, but stronger polar

end group (CNCOO) shows only SmA^* phase [22]. Antiferroelectric phase was reported in an achiral bent-core molecule containing 2,3-difluorotolane unit when its protonated analogue did not show liquid crystalline phase at all [23]. Formation of cholesteric and blue phase is reported in molecules containing 1,4-tetrafluorophenylene units [24]. A fluorosubstituent at the chiral centre [25] or partially fluorinated chain [15,26] results in enhancement in spontaneous polarization (P_s)**.** Effect of fluorination on the relaxation and switching behavior of para, ferro and antiferroelectric liquid crystals has been discussed by many authors [16, 17, 27-30]. Rigidity of the core structure, nature of chirality and extent of fluorination of the constituent molecules are found to have pronounced effect on the collective mode relaxation behavior of room temperature FLC mixtures [29]. A fairly recent review by Michael Hird [8] 'introduces the phenomenon of ferroelectric liquid crystals and charts the development of the technology to commercially viable devices, with a specific focus on the development of suitable materials in terms of design, synthesis and properties' wherein effect of fluorination has also been discussed in detail for both the achiral and chiral systems. Keeping this in view two recently synthesized ferroelectric liquid crystal compounds viz., (S) – (+)-4'-[3-(nonafluoropentanoyloxy) prop-1-oxy]biphenyl-4-yl 4- (1-methylheptyloxy) benzoate and (S)–(+)- 4'-[6-(nonafluoropentanoyloxy) hexyl-1-oxy]biphenyl-4-yl 4-(1-methylheptyloxy) benzoate (code 4F3R and 4F6R, first and second numbers respectively being the number of C atoms in the perfluorinated chain and oligomethylene spacer) [14] has been investigated in detail by X-ray diffraction, dielectric spectroscopy and electro-optic methods.

From small and wide angle X-ray diffraction study the nature of temperature dependence of layer thickness and tilt angle in different phases have been determined. Tilt angle has also been measured by optical methods. It has been discussed in chapter 2 that dielectric spectroscopy studies on ferroelectric liquid crystals are important since one can get information about the relaxation modes directly associated with ferroelectricity [31]. Since the two compounds possess ferroelectric SmC^* phase, one also having SmC^*_A phase, two types of collective relaxation modes may be associated with them, viz., Goldstone mode and Soft mode which can be examined by dielectric relaxation spectroscopy. The Goldstone mode appears in the SmC^* phase because of the phase fluctuations in the azimuthal orientation of the molecular director and its characteristic frequency is usually less than 10 kHz. The soft mode, on the other hand, appears in the neighbourhood of SmA^*- SmC^* transition due to fluctuations in the tilt angles of the molecules.

Both these modes are called collective mode since they represent collective behaviour of the molecules under the influence of an ac field. As the Goldstone mode dielectric increment is usually large compared to the soft mode increment, sometimes it is difficult to study the soft mode properties in the SmC^* phase. Yet, this problem can be overcome by applying a DC electric field in the SmC^* phase, so-called the bias field, being strong enough to unwind the helical arrangement of the polarization vector. In such situation the Goldstone mode is suppressed and the soft mode can be studied almost separately. Although Goldstone mode dielectric increment is usually large compared to the soft mode increment but soft mode critical frequency is at least two orders higher than that of GM. Moreover, according to the generalized Landau model [32] GM critical frequency remains almost independent of temperature whereas that of SM is strongly temperature dependent being associated with the tilt fluctuation of the directors.

In antiferroelectric liquid crystalline (AFLC) materials double relaxation processes with critical frequencies in the kHz and MHz range are usually observed. The low frequency mode (P_L), known as the antiferroelectric mode, is the result of collective reorientation of the molecules in the same direction. The high frequency mode (P_H), known as the antiphase antiferroelectric mode, arises due to collective reorientation of the molecules in the opposite direction [33,34].

Along with frequency-dependent dielectric study spontaneous polarisation (P_S), which is a measure of order parameter and on which the switching time of ferroelectric liquid crystalline (FLC) display devices depends, has also been measured. The rotational viscosity and switching time were also determined to probe the suitability of the materials in display applications.

5.2 COMPOUNDS STUDIED

Molecular structures of the investigated fluorinated ferroelectric compounds and their abbreviated names and transition temperatures (in ^{O}C) are given in the Table 5.1.

Table 5.1: Molecular structures and transition temperatures of the compounds 4F3R and 4F6R

Name	Molecular structure with transition temperature
4F3R	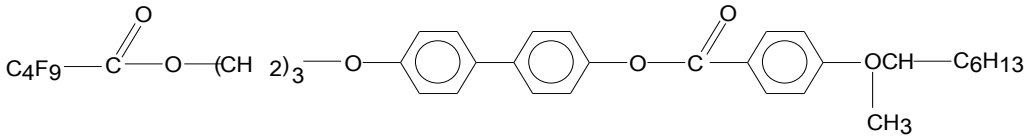 Cr 79.8°C SmC* 134.1°C I
4F6R	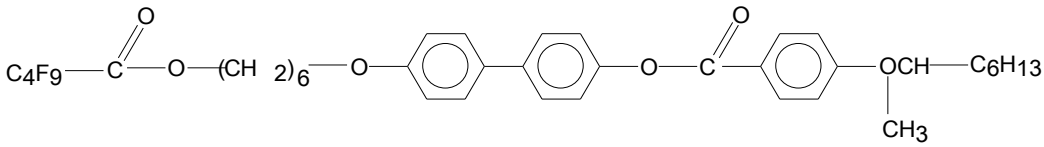 Cr_1 46.7°C Cr_2 60.0°C SmC_A* 86.5°C SmC* 128.3°C I

5.3 EXPERIMENTAL METHODS

The Phase behaviour of the compounds was investigated by polarizing microscope equipped with the heating stage. The heating and cooling rate was 1°C / min and the measurement accuracy was ± 0.1°C. Small and wide angle X-ray scattering measurements (SAXS and WAXS) on randomly oriented samples were made using Ni filtered CuKα radiation and a custom built high temperature camera and photographs were analyzed to find average intermolecular distance and layer spacing. Tilt angles (θ) were calculated using the relation $\theta = \cos^{-1}(d/L)$, where L is the most extended length of the molecules found by geometry optimization.

To perform the dielectric and electrooptic measurements polyimide-coated planar glass cells with low resistivity (about 20Ω/□) indium tin oxide (ITO) electrodes of 4.2 µm cell gap and active electrode area 1.2x0.7 cm^2 were used. Cells were filled by capillary action with samples in isotropic state. Very slow regulated cooling of the sample yielded proper alignment. Complex

dielectric permittivity was measured using a Hewlett-Packard impedance analyzer HP 4192A in the frequency range from 100 Hz to 13 MHz. Automatic data acquisition arrangement was made using RS232 interfacing with a PC.

Spontaneous polarization (P_S) was measured as a function of temperature by the reversal current method [29] using a triangular wave at 10 Hz. The amplitude of the applied voltage was 20Vpp. An oscilloscope was used to record the voltage drop across a resistor in series with the cell as a function of time. The area under the curve was determined from the stored image after creating an appropriate base line following procedure described in chapter 2. Optical tilt of molecules in smectic layers was determined by measuring the angle of rotation of the analyzer between two extinction conditions while the sample was observed under a polarizing microscope in switching condition under a square wave of very low frequency (about 10 MHz). Response time of the sample was determined by measuring the time delay of occurrence of polarization bump from the applied square pulse edge (20Vpp, 10 Hz) while monitoring, in storage oscilloscope, the voltage across a resistor in series with the cell. Sample temperature was regulated by a Eurotherm controller 2216e within ± 0.1^{o}C in all measurements. Details of experimental procedure have already been discussed in chapter 2.

5.4 RESULTS AND DISCUSSION

The compound 4F3R exhibits only synclinic ferroelectric SmC^* phase over a considerable temperature range (ΔT = 54.3^{o}) whereas the compound 4F6R exhibits both SmC_A^* phase (ΔT = 26.5^{o}) and SmC^* phase (ΔT = 41.8^{o}) at the cost of range of SmC^* phase compared to 4F3R. 4F6R also shows two crystalline modifications. Observed textures in different phases for the two compounds are shown in Figure 5.1. Beautiful broken fan shaped texture with clear sign of helicoidal structure in the form of equisdistant parallel lines are observed in SmC^* phase of the first compound. In 4F3R measured enthalpies at the two transitions are 26.47 kJ/mol and 7.11 kJ/mol whereas in 4F6R these are 17kJ/mol, 15.78kJ/mol, 0.01kJ/mol and 7.75kJ/mol respectively [14]. Thus melting and clearing transitions in both the compounds are of first order; however anti-ferroelectric to ferroelectric transition is second order. Phase sequence similar to 4F3R was also observed in homologues with 3, 5 and 6 carbon atoms in the perfluorinated terminal chain [14]. Another important feature of these compounds is that they show direct

transition from the SmC* to isotropic phase, which is rare in FLC materials. It is also found that the compounds are useful for formulation of room temperature FLC mixture as discussed later.

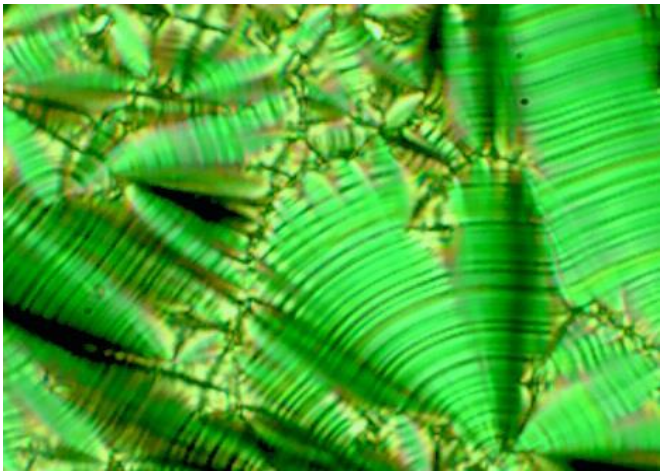

SmC* phase of 4F3R (102°C)

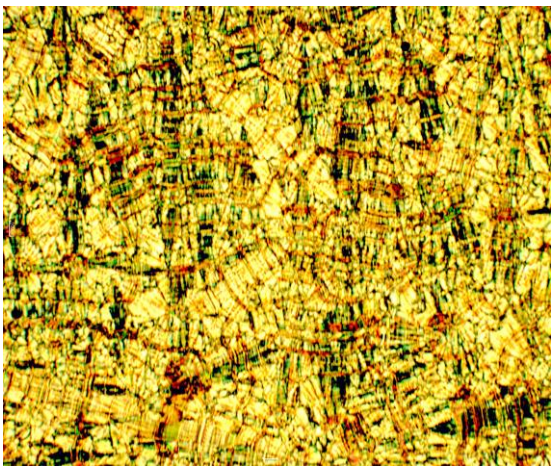

SmC* phase of 4F6R (120°C)

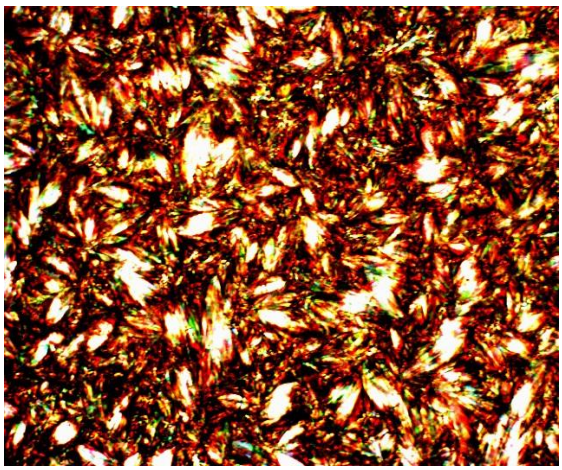

SmC_A^* phase of 4F6R (75°C)

Figure 5.1: Textures in different phases of compounds 4F3R and 4F6R

5.4.1 Optimized Geometry Using Molecular Mechanics

To elucidate the structure of the molecules, 4F3R and 4F6R, their geometry were optimized using PM3 molecular mechanics method in *Hyperchem* software package [35]. While optimizing the geometry the bond, angle and torsional interactions were considered in the force

field along with the van-der Waals and electrostatic interactions. The optimized structures of the molecules of the two compounds, direction of principal axes along with the direction of its electric dipole moment are shown in Figure 5.2. Optimized lengths of the molecules, dipole moments along with their components along the directions of the principal moments of inertia and the corresponding moments of inertia values along the three principal moments of inertia axes are shown in the Table 5.2. Moments of inertia values in 4F6R are significantly higher than those of 4F3R as expected. Dipole moment of 4F6R is also found to be substantially higher than that of 4F3R which is a result of change in molecular conformation due to the increased chain length. Major increase of dipole moment is in the y-component, which is transverse to the molecular long axis satisfying the criteria of presence of transverse dipole moment in the constituent chiral molecules in a tilted smectic phase for the occurrence of ferroelectric phase.

Table 5.2: Optimized length, dipole moment and moments of inertia of 4F3R and 4F6R

Compound	**Optimized Length (Å)**	**Dipole Moment (Debye)**	**Moments of Inertia ($\times 10^{-46}$ kg m^2)**		
			I_{XX}	**I_{YY}**	**I_{ZZ}**
4F3R	33.4	4.25 (-1.98, 3.67, -0.81)	680.3	11576.2	11924.4
4F6R	38.3	5.68 (-2.62, 4.99, 0.67)	3440.9	97612.7	99964.8

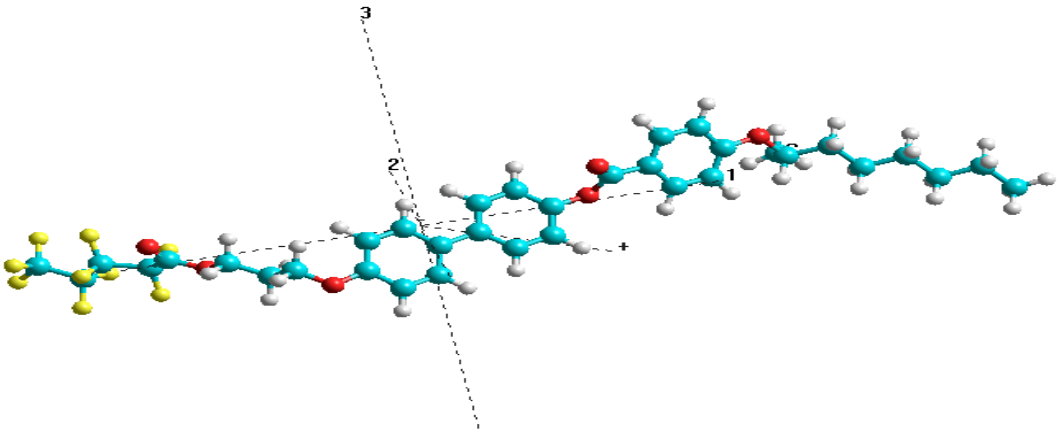

Figure 5.2(a): Optimized geometry of 4F3R

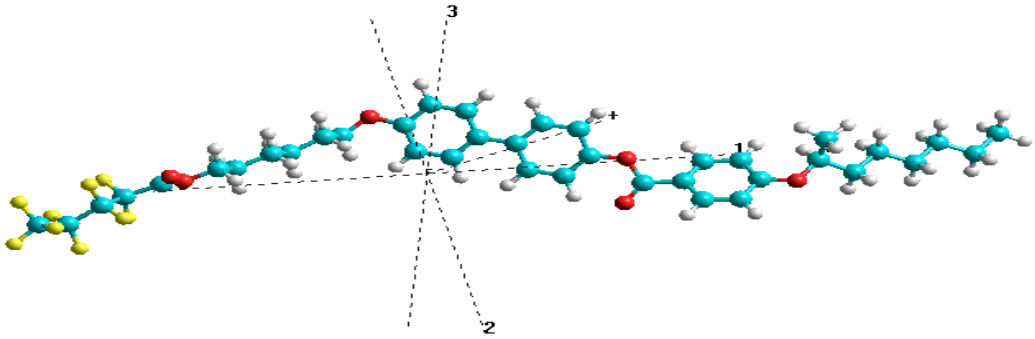

Figure 5.2(b): Optimized geometry of 4F6R

5.4.2 SAXS and WAXS Measurements

Two major diffraction features were observed in the X-ray photographs of randomly oriented sample. Diffused inner ring is related to the layer spacing (d) of the tilted smectic phase and diffused outer ring arises due to interaction of the neighboring molecules in a plane

perpendicular to the molecular axis providing average intermolecular distance (D). X-ray diffraction photographs observed in different phases of the compounds are shown in Figure 5.3.

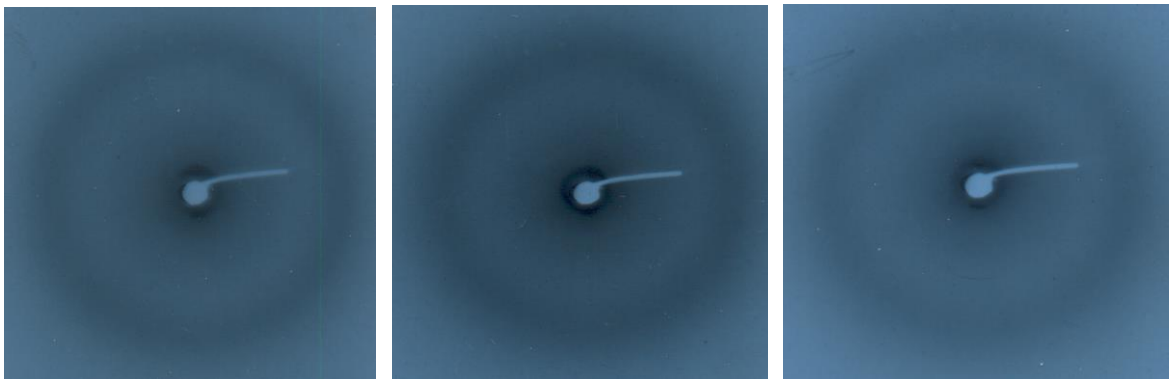

4F3R (110°C) (SmC*) 4F6R (70°C) (SmC$^{*}_{A}$) 4F6R (100°C) (SmC*)

Figure 5.3: X-ray diffraction photographs in different chiral smectic phases of 4F3R and 4F6R

Temperature variations of average intermolecular distance and layer spacing are shown in Figure 5.4 and Figure 5.5. The figure shows that the average intermolecular distance remains almost constant and no discontinuity is observed at SmC$_A^*$ to SmC* transition in 4F6R. At 110°C in SmC* phase, observed D in 4F3R is 5.87 Å while in 4F6R it is 6.89 Å. This considerable increase in D is a result of increased oligomethyline spacer group. The D values obtained in these compounds are also found to be larger than that observed (5.60 Å) in a nematogenic terphenyl compound having fluorine atom connected to the opposite side of a phenyl ring [36] and may be due to the presence of the bulky chiral –CH$_3$ group, the oligomethyline spacer and the ester bridge between the two phenyl rings. Present observation on D is consistent with other previous reported data [37,38]. Layer spacing (d) observed in 4F3R shows nonlinear increasing trend with temperature while in 4F6R it shows linear increasing trend in both ferroelectric and antiferroelectric smectic phases but observed d values are higher in SmC* phase than in SmC$_A^*$ phase. However, in this case clear discontinuities are observed at SmC$_A^*$ – SmC* transition. In 4F3R, the layer spacing increases from 23 Å (79 ^{o}C) to 28.6 Å (129 ^{o}C) where as in 4F6R, d increases from 28.5 Å (64 ^{o}C) to 33 Å (84 ^{o}C) in SmC$_A^*$ phase and further increases from 34.7 Å (89 ^{o}C) to 38.8 Å (124 ^{o}C) in SmC* phase. Increased layer spacing is a result of decrease of tilt angle of the molecules with respect to the layer normal, if it is assumed that the molecules behave as rigid rods and molecular conformations do not change appreciably with temperature.

Similar variation of layer thickness with temperature is observed in related homologues of the series [14]. It is worth of mention that nonlinear increase of d with temperature had also been reported in both ferroelectric SmC^* and antiferroelectric SmC^*_A phases from synchrotron X-ray diffraction [39]. Continuous layer expansion on lowering of temperature or almost temperature independent layer spacing (hence free from chevron defects) had also been observed in pure or FLC mixtures [40].

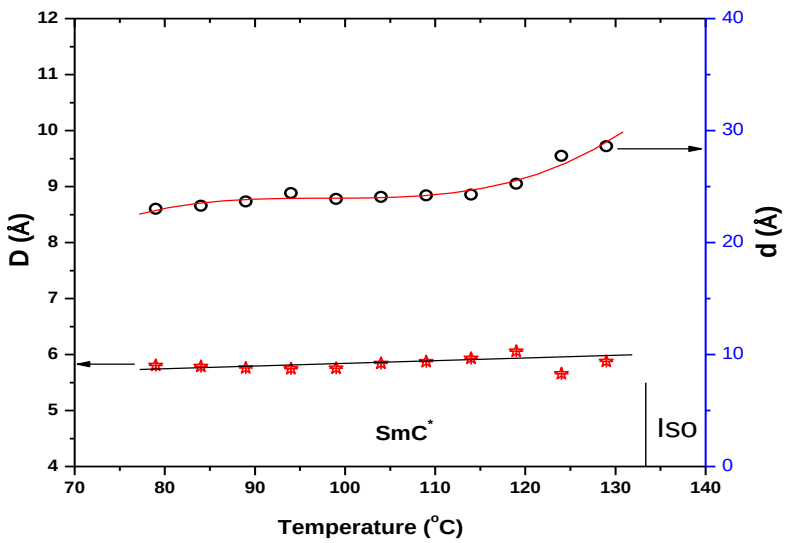

Figure 5.4: Variations of average intermolecular distance (D) and layer spacing (d) with temperature in 4F3R

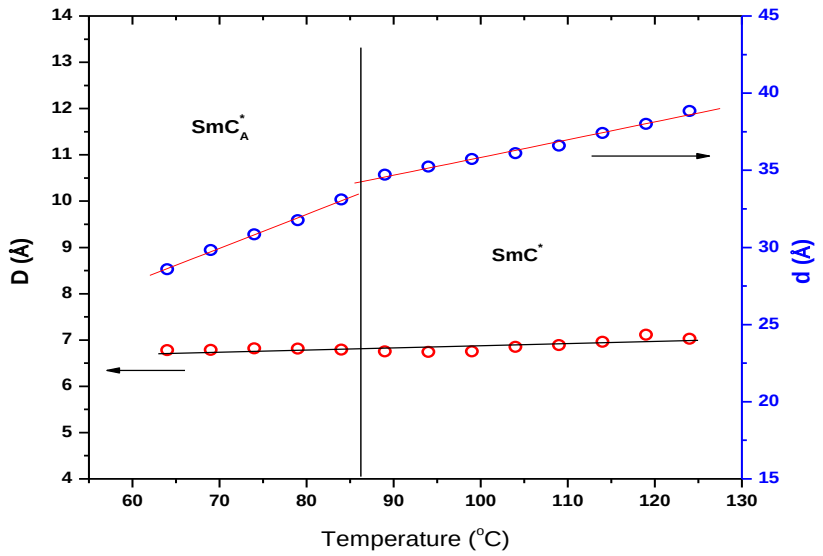

Figure 5.5: Variations of average intermolecular distance (D) and layer spacing (d) with temperature in 4F6R

The tilt angle (θ) of the molecular directors, often referred to as primary order parameter of FLC phase, was calculated under rigid rod approximation, estimated error in tilt angle being $\pm 0.5^0$. In both the compounds tilt angles were found to decrease with temperature as shown in Figure 5.6 and Figure 5.7. In 4F3R at 84°C tilt angle was found to be 45.5° which decreases to 30.9° at 129°C while in 4F6R at 64°C tilt angle was found to be 42.1° which decreases to 30.2° at 124°C. Thus both the compounds may behave as orthoconic antiferroelectric liquid crystals. Slight discontinuity in tilt is observed at SmC^*_A to SmC^* transition in 4F6R. Tilt angles were also determined optically and have also been depicted in Figure 5.6 and Figure 5.7 for comparison with X-ray tilt. Optical tilts reflect the angle between the direction of molecular core and the layer normal, since the principal axis of indicatrix coincides with the core direction. On the other hand, X-ray tilts determined by the ratio of the layer thickness in SmC^* phase to the most extended molecular length, are related to the average direction of total populations of electrons of the molecules. Moreover, it is difficult to ascertain the effect of change in molecular conformation in the FLC phase on the most extended molecular length in an isolated molecule. Thus X-ray tilt is usually found to be larger than optical tilt, which is found to be true in both the compounds. On the other hand, in a structurally similar compound with only an additional

carboxylate group in between the phenyl group and the chiral centre, the optical tilt was found to be near 45^0 and higher than that calculated from small-angle X-ray diffraction [41,42]. It might be mentioned here that high tilt materials are suitable for total internal reflection based microoptic switch for multimode fiber and for display devices with gray scale capability under proper surface anchoring condition [43-45].

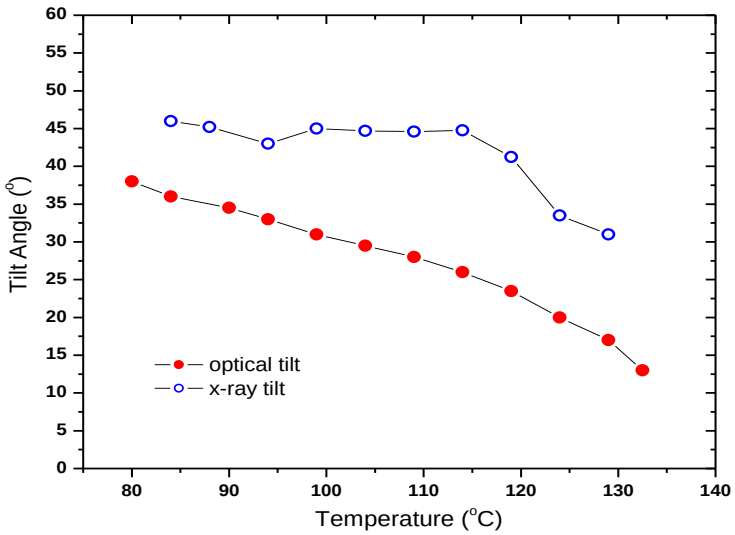

Figure 5.6: Temperature variation of X-ray and optical tilt of 4F3R

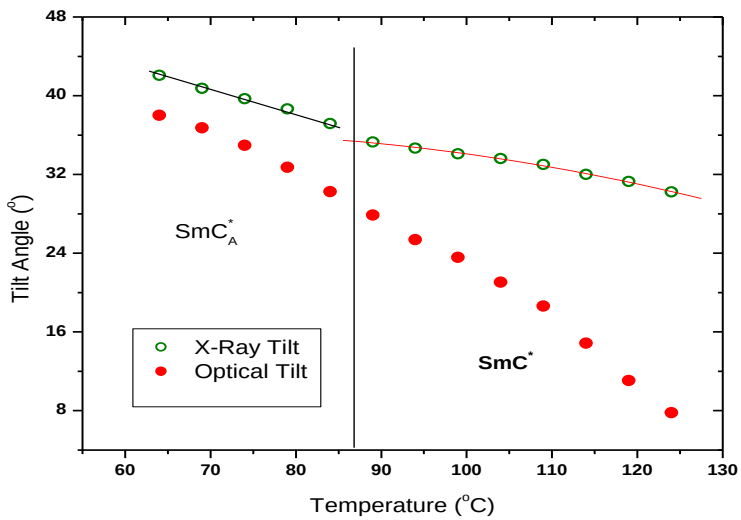

Figure 5.7: Temperature variation of X-ray and optical tilt of 4F6R

5.4.3 Frequency dependent dielectric relaxation study

Observed real ($\varepsilon^{/}$) and imaginary ($\varepsilon^{//}$) parts of dielectric constants as function of frequency at different temperature for the two compounds are shown in Figure 5.8 and Figure 5.9. As a representative example, dielectric spectra in the SmC* phase fitted to Cole-Cole function for 4F3R is shown in Figure 5.10. Separate contribution of each relaxation mode and conductivity are also shown in the figure along with the fitted parameters. Since real and imaginary parts of dielectric constants are related through Kramers-Kronig relations, Cole-Cole plot of the same data is shown in Figure 5.11, which shows that the fitting was good. Only one absorption peak (strong in 4F3R than in 4F6R) was observed in SmC* phase which was found to be suppressed when a bias voltage of 15 Volt was applied. This absorption process is, therefore, definitely associated with GM relaxation mode. Absorption peak at around 600 kHz was observed at all temperatures which were presumed due to ITO. No SM process is observed, even when a dc bias field was applied in addition to the measuring field, due to non-existence of SmA* phase in the two compounds. It is very unlikely that coincidence of SM critical frequency with ITO mode at all temperatures even with bias is the cause for non-observance of SM. It is clear from the figure that only GM relaxation was observed in the ferroelectric phase which persists in the antiferroelectric phase.

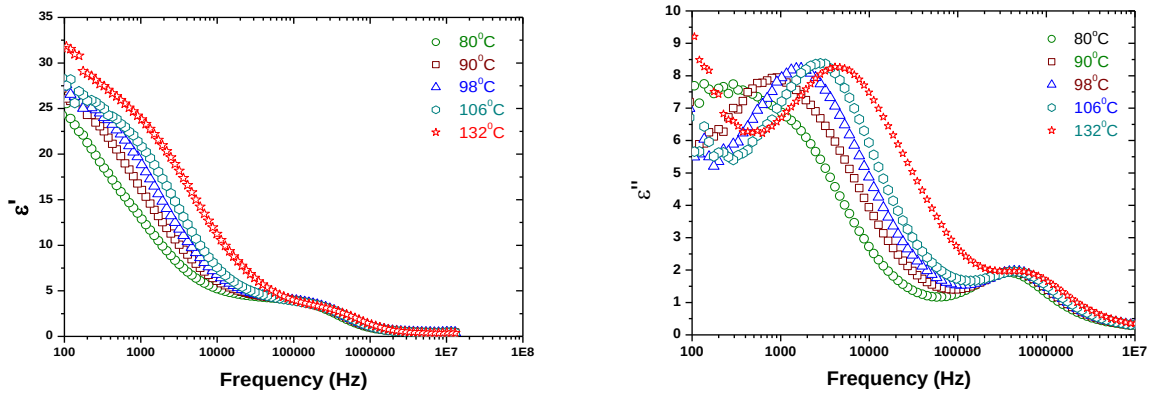

(a) (b)

Figure 5.8: (a) Real ($\varepsilon^{/}$) and (b) imaginary part ($\varepsilon^{//}$) of dielectric constant as function of frequency at selected temperatures of 4F3R

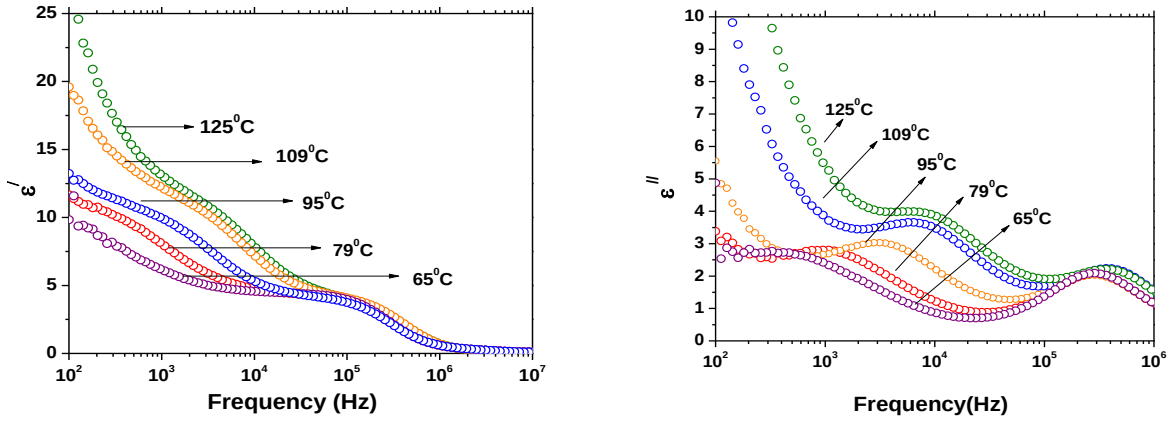

(a) (b)

Figure 5.9: (a) Real ($\varepsilon^{/}$) and (b) imaginary part ($\varepsilon^{//}$) of dielectric constant as function of frequency at selected temperatures of 4F6R

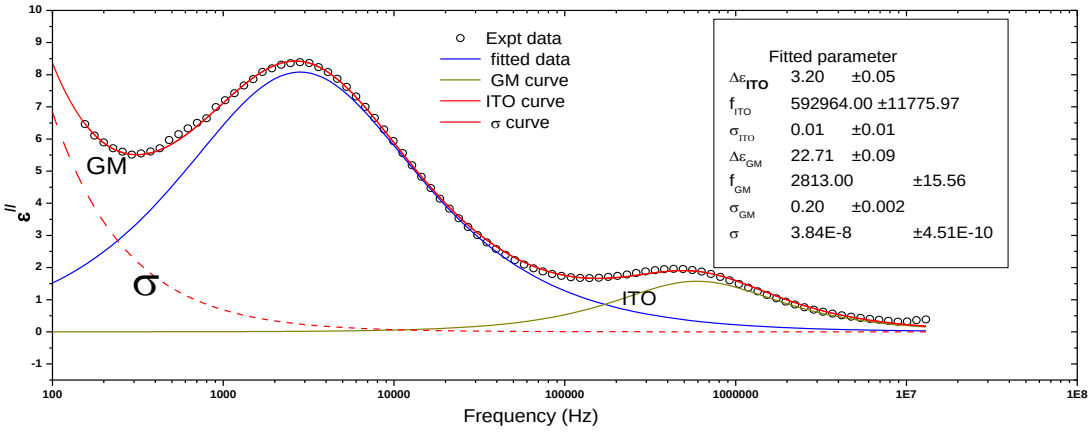

Figure 5.10: Fitted spectra in SmC* phase (106^0C) of 4F3R along with observed data. GM, ITO and σ curves are also shown separately along with fitted parameters

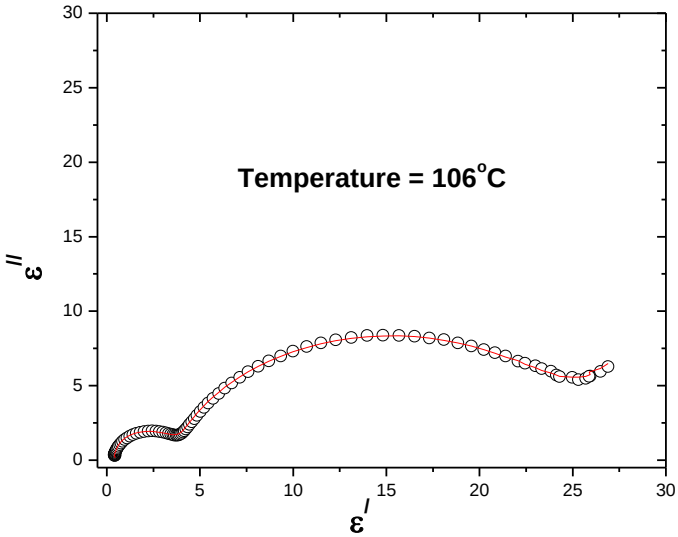

Figure 5.11: Cole-Cole plot of 4F3R

From the Landau model concept of soft mode was first introduced to the SmA*-SmC* phase transition by Blinc and Zeks [46] for the case of a modulated structure and later modified

by Carlsson *et al.* [47] where phase transition was described in terms of two order parameters – two-component tilt vector as primary order parameter and two-component in-plane polarization as the secondary order parameter. Two characteristics modes are observed in SmA*-SmC* second order phase transition where the continuous symmetry group of SmA* (D_∞) is spontaneously broken in SmC*(C_2). Whereas the soft mode is a symmetry breaking mode, which critically slows down (softens) on approaching the phase transition from above; the Goldstone mode is zero frequency mode that tries to restore the broken symmetry. Thus soft mode splits into the phase (GM) and amplitude (SM) modes in SmC* near the transition. According to Clark and Lagerwall [48], in majority of the reported cases, SmC^* phase is formed by cooling from the SmA^* phase through a second-order phase transition, whereas when SmC^* phase is created directly from the nematic or from the isotropic liquid phase, layers of tilted molecules have to appear directly at the transition, which makes the transition first order. Since in the present compounds SmC* phase is created directly from isotropic phase, nature of phase transition is first order (as is revealed from the clearing point enthalpy and temperature dependence of both the primary and secondary order parameters), so theoretically no soft mode is expected which is confirmed by the present experiment. This is further supported by the fact that a higher homologue of the series viz., 7F3R which forms SmA^* on heating the SmC* phase exhibits soft mode relaxation behaviour [49]. For two reasons it may not be proper to argue that the absence of SmA* phase is only because of the fluorinated ester unit in the achiral terminal chain of the molecules. First, from reference 15 it is observed that three other homologous members (1F3R, 2F3R AND 7F3R) of the present compounds also exhibit SmA* phase and second, another series of compounds having same rigid core but with achiral alkoxy chain exhibit N* phase above SmC* [50]. Rather the conformational change of the molecules especially with respect to the fluorinated ester unit having intervening oligomethylene spacer and consequence change in the dipole-dipole interaction between the molecules is probably the reason for the destabilization of SmA* phase and hence the absence of the soft mode in the dielectric relaxation behaviour.

Moreover, under a strong bias field, appearance of a residual mode usually at higher frequency, known in literature as domain mode [51–53] is also discussed for compounds having Ps > 50 nC/cm^2, but no such mode is observed in the present case. This may be due to less Ps in the present compounds discussed below. It is also not clear whether presence of SM in SmC* and SmA* phases is a prerequisite for the detection of the domain mode, because in all the above

referred compounds SM was present in both the phases. As transitional effect, phase fluctuation is found to persist a few degrees above SmC*-I transition in the dielectric spectra. However, in the crystalline phase only ITO absorption peak is observed in the studied frequency window, signifying complete freezing of molecular motions.

Variations of dielectric increment and relaxation frequency as function of temperatures are shown in Figure 5.12 and Figure 5.13 for the compounds 4F3R and 4F6R respectively. A sharp discontinuity in $\Delta\varepsilon$ is observed at SmC_A^* – SmC^* transition as expected, but magnitude of $\Delta\varepsilon$ in SmC_A* phase is quite large (~ 6) which is usually of the order of one or at the most two as reported in literature for typical SmC_A* [54-56] or for its variant like SmC_A*(1/3) and SmC_A*(1/2) phases [57]. Repetition of relaxation experiments with different cells confirmed the above observation. It is not possible to give any definite explanation for this, however, it may be thought that due to surface interactions under the confined geometry of thin dielectric cell (4.2 μm), the material is probably showing ferrielectric type behavior although in bulk it shows antiferroelectric phase. This is supported by the fact that in SmC_A^* phase only GM like absorption mode is observed instead of low frequency P_L and high frequency P_H modes which are usually observed in SmC_A^* phase. Dielectric increment ($\Delta\varepsilon$) is found to increase considerably with temperature. In compound 4F3R it increases from 15.1 (80^0C) to 25.8 (132^0C), rate of increment is faster up to 110^0C, where as in 4F6R it increases from 5.62 (61^0C) to 6.51 (85^0C) in SmC_A^* phase and further increases from 9.06 (87^0C) to 12.93 (127^0C) in SmC^* phase. Such increase has been reported in several FLC compounds [58-60]. Increase of dielectric strength with temperature in SmC^* may be explained if one assumes stronger biquadratic coupling between tilt and polarization compared to bilinear one in the expression for free energy density in generalized Landau model [32]. But in such situation, $\Delta\varepsilon$ should decrease near transition temperature (T_c), which is not observed in the present study. Moreover, critical absorption frequency (f_C) is also found to increase considerably with temperature. Observed f_c for 4F3R increases from 331 Hz to 4751 Hz, where as for 4F6R it increases from 181Hz to 6738Hz. However, for both the compounds near SmC^*-I transition f_C decreases slightly. In the literature both temperature independent f_c [53,58,59,61,62] and increase of f_c with temperature [60,63,64] are reported in pure and FLC mixtures. Although according to generalized Landau model critical frequency (f_c) of GM does not depend on temperature unlike that of SM which depends linearly

on ($T-T_C$), GM critical frequency depends on modified elastic constant (K_Φ) and rotational viscosity (γ_G) of azimuthal motion and wave vector (q) of the helical pitch ($q=2\pi/p$, p=pitch of helix) in accordance with the relation $f_c = K_\Phi q^2 / (2\pi\gamma_G)$, it is expected that f_c will somehow depend on temperature as K_Φ, γ_G and q are functions of temperature.

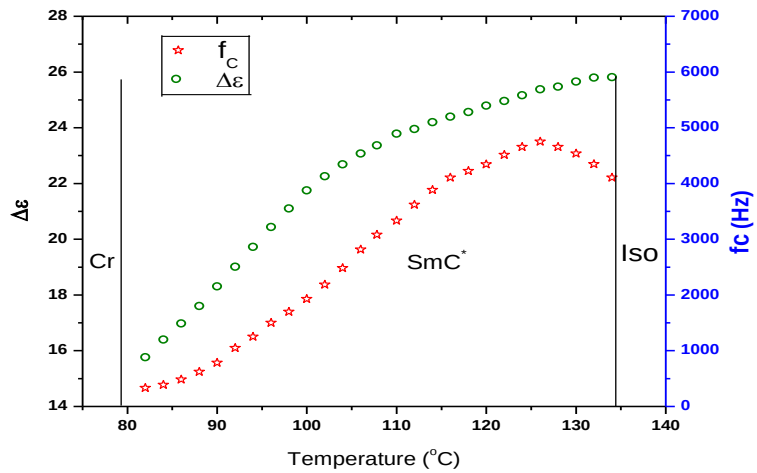

Figure 5.12: Variation of dielectric increment (Δε) and Goldstone mode relaxation frequency (f_c) as a function of temperature for 4F3R

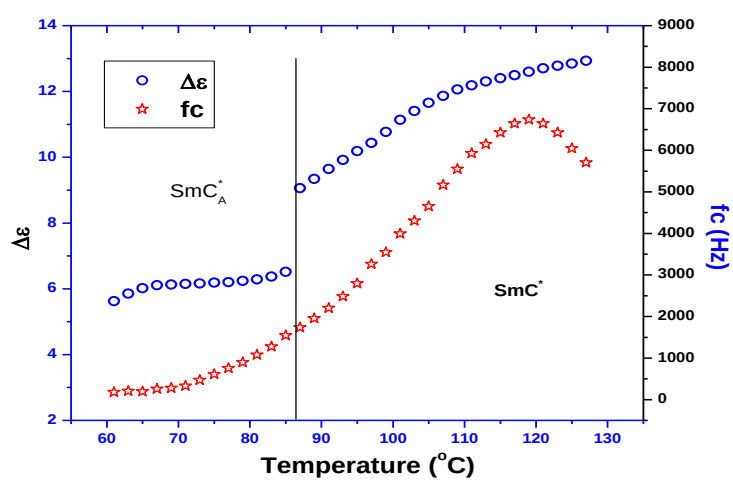

Figure 5.13: Variation of dielectric increment (Δε) and Goldstone mode relaxation frequency (f_C) as a function of temperature for 4F6R

Strength of the absorption is found to be nearly constant (around 8) throughout the ferroelectric phase of 4F3R whereas in 4F6R it varies in between 3-5. Much stronger absorption (about 35) was reported in $C_6F_{13}CH_2CH_2O$-Ph-Ph-COO-Ph-COO-CH(CH_3)C_6H_{13} and $C_5H_{11}COO(CH_2)_6$-O-Ph-Ph(2' 3' F)-Ph-COO-CH(CH_3)-C_6H_{13} [65,60]. Thus the investigated compounds will absorb, over a frequency range of a few hundred hertz to a few thousand hertz, far less energy from the input signal compared to the above two similar compounds.

5.4.4 Spontaneous Polarization

Spontaneous polarisation (P_S) was measured as a function of temperature. The input triangular pulse and output signal across a standard resistance in series with the liquid crystal cell captured in a digital oscilloscope are shown in Figure 5.14. From the polarization peak area P_S was calculated. P_S in the low temperature regime of SmC^* phase is about 8 nC/cm^2 higher in 4F6R compared to 4F3R. This is expected since 4F6R possess higher dipole moment. As depicted in Figure 5.15 and Figure 5.16, spontaneous polarization decreases slowly with temperature for both the compounds. In 4F3R it is found to decrease from 41.66 nC/cm^2 (75°C) to 16.66 nC/cm^2 (138°C) where as in 4F6R it decreases from 51.26 nC/cm^2 (61°C) to 17.28 nC/cm^2 (127°C). P_S values of this range is within acceptable limits for various applications especially from the point of switching time [29,66]. No discontinuity at the SmC_A^*–SmC^* transition was observed, similar behaviour has been reported in other AFLCs [67].

For comparison it may be pointed out, compounds with similar backbone, only with different fluorinated carboxylate chain (Viz. C_4F_9COO-$(CH_2)_6$ and $C_5F_{11}COO$-$(CH_2)_6$) exhibit P_S of about 50 nC/cm^2 near Cr-SmC^* transition but when longer fluorinated chain $C_8F_{17}COO$-$(CH_2)_2$ is introduced P_S increases to about 93 nC/cm^2 [14]. On the introduction of another carboxylate group in between the phenyl group and the chiral centre, P_S drastically increases to above 200 nC/cm^2 [12,65]. A partially fluorinated terphenyl based AFLC compound [$C_5F_{11}COO$ $(CH_2)_6$-O-Ph-Ph(2' 3' F)-Ph-COO-CH(CH_3)-C_6H_{13}] showed P_S value 118.7 nC/cm^2 [60]. Thus both the core structure and chain length have pronounced effect on the magnitude of spontaneous polarization.

(a)

(b)

Figure 5.14: Input and output signals captured in a digital oscilloscope for (a) 4F3R and (b) 4F6R

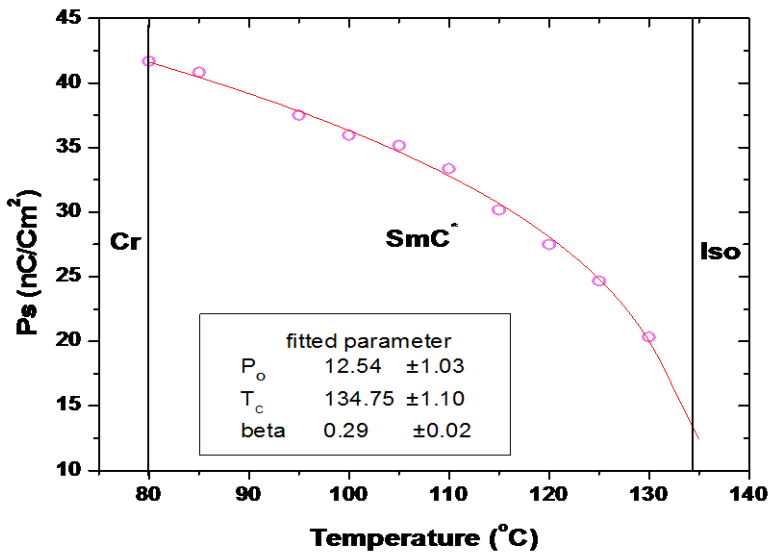

Figure 5.15: Temperature dependence of P_S of 4F3R. Mean field fitted curve is also shown

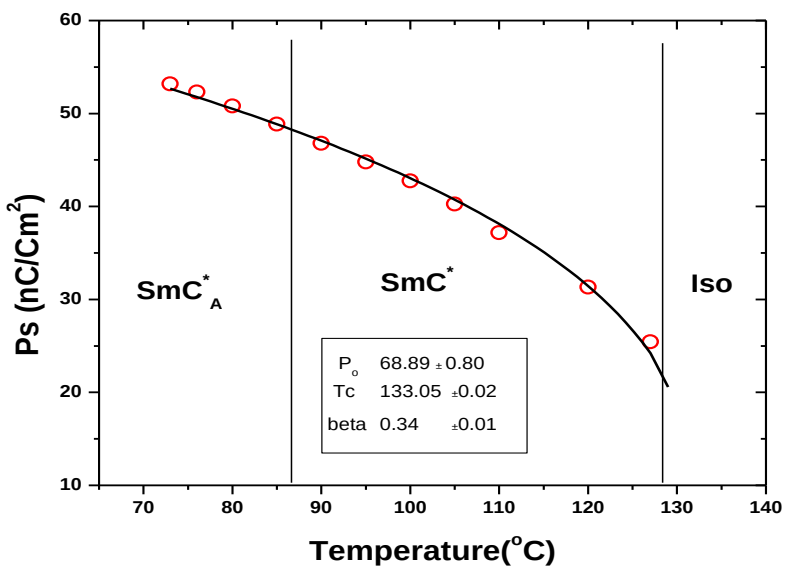

Figure 5.16: Temperature dependence of P_S of 4F6R. Mean field fitted curve is also shown

Moreover, measured P_S data were found to fit nicely to the mean-field model $P_S=P_0\,(T_C - T)^{\beta}$ where T_C is the SmC* to isotropic transition temperature and β is the critical exponent for the secondary order parameter P_S [68]. In 4F3R fitted T_C was found to be within 0.5 degree of the

observed critical temperature whereas it is within 5 degree in 4F6R. However, fitted β-value for the two cases are found to be 0.29 and 0.34 which deviate significantly from the mean field value (0.5), signifying the SmC^* to isotropic transition is not second order in nature according to Ehernfest's classification, rather it is strongly first order. Observed change in enthalpy at SmC*-I transition supports this view. Similar observation was reported before in ferroelectric phases of epoxy compounds [69]. As noted before this is also consistent with the general observation by Clark and Lagerwall [48] that when SmC^* phase is created directly from the nematic or from the isotropic phase, layers of tilted molecules have to appear directly at the transition, which makes the transition first order.

5.4.5 Rotational Viscosity and Activation Energy

Rotational viscosity (γ_Φ), which is related to rotations of the molecular directors about the SmC^* cone, is one of the most important parameters of the SmC* phase and strongly influences the switching time between the field-induced states of FLCs. Rotational viscosity (γ_Φ) was determined using the following relationship derived from the generalized Landau model [32]:

$$\gamma_\varphi = \frac{1}{4\pi\varepsilon_0}\frac{1}{\Delta\varepsilon f_c}\left(\frac{P_S}{\theta}\right)^2$$

where Goldstone mode dielectric strength (Δε) and relaxation frequency (f_c) were obtained from dielectric relaxation study and tilt angle (θ) was obtained from SAXS measurements. A similar expression was used to find its value in SmC_A^* for the compound 4F6R. γ_Φ in SmC_A^* phase of 4F6R is about 5 times more than the highest value in SmC^* phase in 4F3R. Thus increased oligomethylene spacer group increases viscosity to a large extent. Variation of γ_Φ with temperature is shown in Figure 5.17 and Figure 5.18 for the two compounds. It is observed that within a span of 10^0C, the rotational viscosity of 4F3R falls to about one fourth of its value near Cr-SmC^* transition, thereafter, it remains almost constant. In 4F6R also viscosity decreases quite fast with temperature in a non-linear manner, rate of decrement is different in antiferroelectric and ferroelectric phases. Moreover, rotational viscosity was found to obey following Arrhenius relationship:

$$\gamma_{\varphi} \propto e^{\frac{E_a}{k_\beta T}}$$

where E_a is the activation energy for the molecular rotation on the cone when the AC field is applied to the FLC material and k_β is the Boltzmann constant. From a linear least squares fit of the plot of ln γ_Φ versus inverse temperature, activation energy was calculated. The activation energies are found to be 97.09 kJ mol^{-1} and 105.04 kJ mol^{-1} in 4F3R and 4F6R respectively. In a terphenyl based AFLC compound [60], the activation energy was found to be 48.14 kJ mol^{-1}, which is almost half of the activation energy of 4F3R. Optimizing the geometry of the above AFLC compound using Hyperchem it is found that its dipole moment is only 1.70 D, considerably less than the dipole moment of 4F3R (4.25D) and 4F6R (5.75D). Stronger dipole-dipole interaction between molecules of 4F3R and 4F6R may be responsible for higher activation energy.

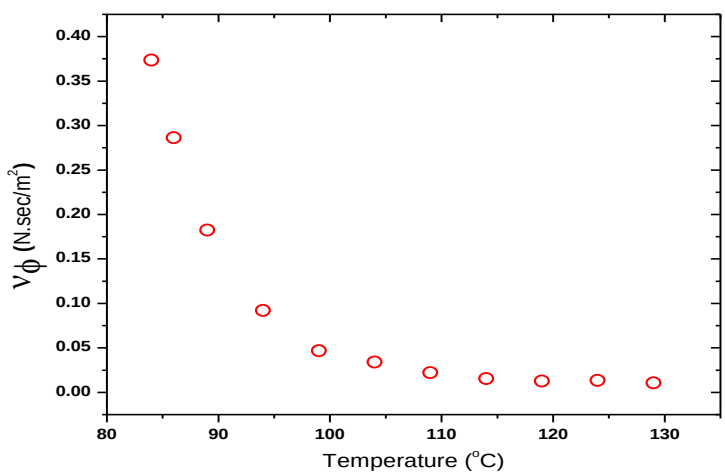

Figure 5.17: Variation of rotational viscosity (γ_Φ) with temperature of 4F3R

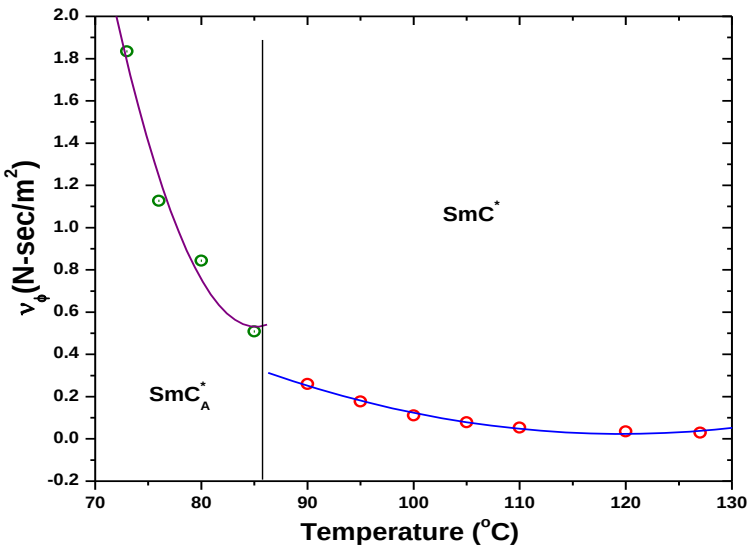

Figure 5.18: Variation of rotational viscosity (γ_Φ) with temperature of 4F6R

5.4.6 Response Time

Electrical response time is a very important parameter for a display device. It is basically the time taken by the liquid crystalline samples to respond to an external electrical pulse. The compounds show very fast switching. The low value of electrical response time is basically due to the large Ps and low rotational viscosity possessed by the compounds. In 4F3R the response time varies from 24-88 µs in SmC^* phase, whereas in 4F6R it varies 235-595 µs in SmC_A^* and 117-223 µs in SmC^* phase. This is expected since the compound 4F6R possesses longer chain length than compound 4F3R which creates more hindrance in switching as well as responding to the external pulse. In other words slower response in 4F6R is due to higher viscosity. Temperature variations of electrical response time are shown in Figure 5.19 and Figure 5.20. It was found to decrease monotonically with increasing temperature, which is due to faster decrease of rotational viscosity (making the rotation of the molecules around the tilt cone easier) compared to spontaneous polarization. At this point it is worth to see how the response time changes with molecular cores and fluorination in chain or core. In a biphenyl based non-fluorinated FLC compound with ester group on both sides of core it was found to be of the order of a few millisecond [70], in a compound obtained with the addition of another mono-fluorinated

phenyl group in the above core structure response time was found to vary between 150-600 µs [62], in a terphenyl based non-fluorinated compound with similar core structure as of 4F3R reported response time is around 3 µs [71], in a terphenyl based fluorinated compound but with different core structure it is reported as 6-22 µs [72] and in a FLC mixture it was found to vary between 25-55 µs [64].

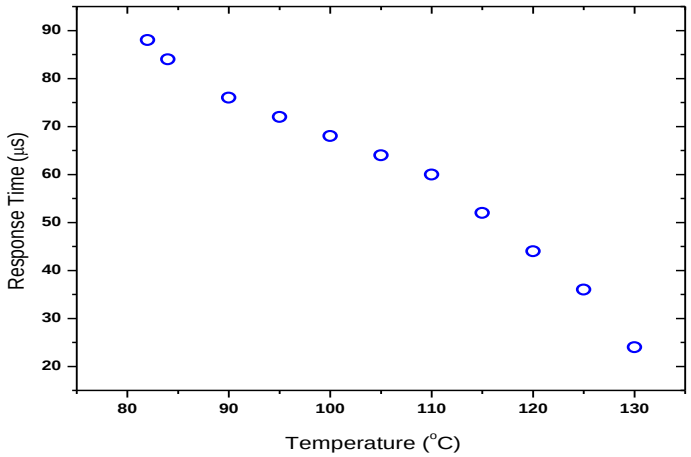

Figure 5.19: Variation of response time with temperature of 4F3R

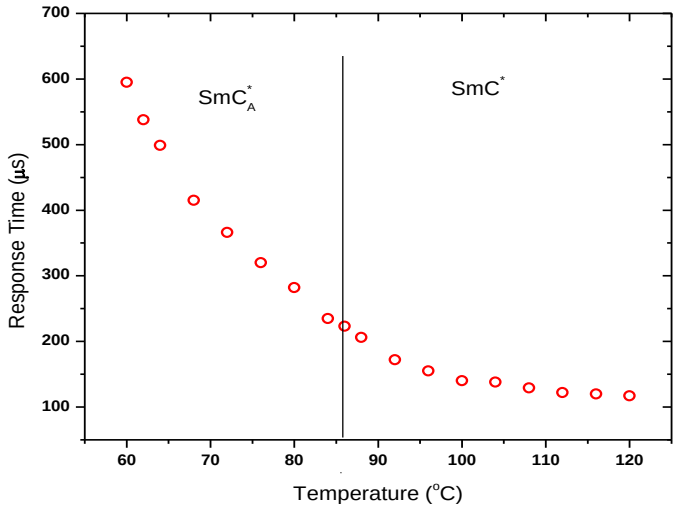

Figure 5.20: Variation of response time with temperature of 4F6R

5.5 ROOM TEMPERATURE MIXTURE FORMULATION

Although ferroelectric SmC* phase in 4F3R is very broad but it is formed at quite high temperature (79.8^{0}C), situation further deteriorates in 4F6R. In order to get SmC* phase at low temperatures we first formulated a host mixture, having tilted SmC phase, by mixing four phenyl pyrimidine based compounds, of which two exhibit SmC and SmA phases and other two form nematic phase in addition. Phase sequence and transition temperatures of the host mixture was found to be 19ºC SmC 69.4ºC SmA 78.7ºC N 81.2ºC I. Compound 4F3R as dopant could induce ferroelectric SmC* phase in the above host mixture at temperature even below ambient temperature, observed phase sequence being Cr < 12.5ºC SmC* 68.5°C SmA* 88.6°C I. Alignment of the mixture in bookshelf geometry in a display cell will be easier because of the presence of SmA* phase in the mixture above SmC* phase, thus the mixture is expected to be a promising room temperature FLC mixture. The weight percentage of the host compounds along with their transition temperatures are given in the Table 5.3.

Table 5.3: Weight percentage and transition temperatures of host compounds

Name	Structure with Transition Temperature	Weight percentage
Host 1(9OCPO9)	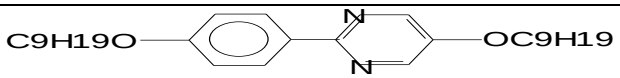 Cr 61.8ºC SmC 95.6ºC SmA 99.1ºC I	20%
Host 2 (7OCPO9)	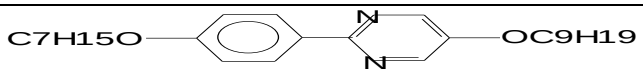 Cr 57.4ºC SmC 95.1ºC SmA 98.4ºC I	20%
Host 3 (9OCPO7)	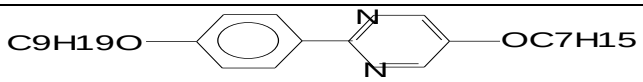 Cr 57.2ºC SmC 79.1ºC SmA 91.2ºC N 94.7ºC I	20%
Host 4 (6OCPO8)	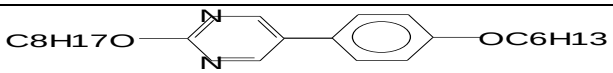 Cr 27.5ºC SmC 46.3ºC SmA 57.5ºC N 65.6ºC I	40%

Mixture Composition: Host (60%) + Dopant 4F3R (40%)

5.6 CONCLUSION

Optical polarizing microscopy, dielectric and electrooptic measurements confirm that the compound 4F3R possesses only ferroelectric SmC^* phase over a broad temperature range whereas compound 4F6R possesses both anti-ferroelectric SmC_A^* phase and ferroelectric SmC^* phase over a considerable temperature range. Both the compounds directly goes to isotropic phase from SmC^* phase which is not common in FLCs. Dipole moment of 4F6R is found to be substantially higher than that of 4F3R which might be the result of change of molecular conformation due increased oligomethylene spacer group. X-ray study reveals that the layer spacing in antiferroelectric and ferroelectric smectic phases show a slightly increasing trend where as average intermolecular distance remains almost constant. Clear discontinuities are observed at SmC_A^*–SmC^* transition in 4F6R while studying the temperature variation of layer spacing, x-ray tilt, dielectric increment and rotational viscosity. Only Goldstone mode relaxation behavior is observed in both the compounds, increase of its dielectric strength and critical frequency with temperature has been explained in the light of generalized Landau model. Fitted data shows that the GM mode is of the Cole–Cole type. No soft mode is observed since the compound directly melts into isotropic phase. The fact that the compounds show quite strong dipole moments, about 45° tilt angle, moderately strong polarization, low viscosity, micro-second range switching and are capable of forming room temperature ferroelectric phase in appropriate host mixture make them suitable from application point of view.

5.7 REFERENCES

[1] R. B. Meyer, Paper presented at the 5th Int. Liquid Crystal Conf., Stockholm, June, (1974); R. B. Meyer, L. Liebert, L. Strzelecki and P. Kelker, J Phys (Paris) Lett.,36, L69 (1975), Ferroelectric liquid crystals.

[2] A. D. L. Chandani, Y. Ouchi, H. Takezoe, A. Fakuda, K. Terashima, K. Furukawa and A. Kishi; Jpn. J. Appl. Phys. Part 2, 28, L1261 (1989), Novel Phases Exhibiting Tristable Switching.

[3] Y. Izozaki, T. Fujikawa, H. Takezoe, A. Fukuda, T. Hagiwara, Y. Suzuki and I. Kawamura, Phys. Rev. B; 48, 13439 (1993), Devil's staircase formed by competing interactions stabilizing the ferroelectric smectic-C* phase and the antiferroelectric smectic-C_A* phase in liquid crystalline binary mixtures.

[4] J. P. F. Lagerwall, D. D. Parghi, D. Kruerke, F. Gouda, and P. Jagemalm, Liq. Cryst., 29, 163 (2002), Phases, phase transitions and confinement effects in a series of antiferroelectric liquid crystals.

[5] J. P. F. Lagerwall, P. Rudquist, and S.T. Lagerwall; Liq. Cryst., 30, 399 (2003), On the phase sequence of antiferroelectric liquid crystals and its relation to orientational and translational order.

[6] E. Gorecka, D. Pociecha, M. Čepič, B. Žekš, R. Dabrowski; Phys. Rev. E, 65, 061703 (2002), Enantiomeric excess dependence of the phase diagram of antiferroelectric liquid crystals.

[7] I. C. Sage, Applications, in: D. Demus, J. Goodby, G.W. Gray, H.W. Spiess, V. Vill (Eds.), Handbook of Liquid Crystals Vol. I – Fundamentals, Wiley-Vch., Weinheim, pp. 731-762 (1998).

[8] M. Hird; Liq. Cryst., 38, 1467–1493 (2011), Ferroelectricity in liquid crystals-materials, properties and applications.

[9] P. J. Collings, Ferroelectric liquid crystals: The 2004 Benjamin Franklin Medal in Physics presented to Robert B. Meyer of Brandeis University, J. Frankl. Inst. 342, 599–608 (2005).

[10] J. Wen, M. Tian, Q. Chen, Liq. Cryst. 16, 445-453 (1994), Novel fluorinated liquid crystals. II. The synthesis and phase transitions of a novel type of ferroelectric liquid crystals containing 1,4-tetrafluorophenylene moiety.

[11] Y. Xu, W. Wang, Q. Chen, J. Wen; Liq. Cryst., 21, 65-71 (1996), Synthesis and transition temperatures of novel fluorinated chiral liquid crystals containing 1,4-tetrafluorophenylene units.

[12] R. Dąbrowski, J. Gąsowska, J. Otón, W. Piecek, J. Przedmojski, M. Tykarska; High tilted antiferroelectric liquid crystalline materials, Disp. 25, 9-19 (2004).

[13] R. Dąbrowski, P. Kula, Z. Raszewski, W. Piecek, J. M. Otòn, A. Spadło; Ferroelectrics, 395 116-132 (2010), New orthoconic antiferroelectrics useful for applications.

[14] D. Ziobro, R. Dąbrowski, M. Tykarska, W. Drzewiński, M. Filipowicz, W. Rejmer, K. Kuśmierek, P. Morowiak, W. Piecek; Liq. Cryst. 39, 1011-1032 (2012), Synthesis and properties of new ferroelectric and antiferroelectric liquid crystals with a biphenylyl benzoate rigid core.

[15] H. T. Nguyen, J. C. Rouillon, A. Babeau, J. P. Marcerou, G. Sigaud; Liq. Cryst. 26, 1007-1019 (1999), Synthesis, properties and crystal structure of chiral semiperfluorinated liquid crystals with ferro and anticlinic smectic phases.

[16] R. Dabrowski, Ferroelectrics, 243, 1-18 (2000), Liquid crystals with fluorinated terminal chains and antiferroelectric properties.

[17] S. Seomun, T. Gouda, Y. Takanishi, K. Ishikawa, H. Takezoe; Liq. Cryst. 26, 151-161(1999), Bulk optical properties in binary mixtures of antiferroelectric liquid crystal compounds showing V-shaped switching.

[18] J. V. Selinger, P. J. Collings, R. Shashidhar; Phys. Rev. E 64, 061705/1-9 (2001), Field-dependent tilt and birefringence of electroclinic liquid crystals: Theory and experiment.

[19] W. M. Zoghaib, C. Carboni, A. K. George, S. AL-Manthari, A. Al-Hussaini, F. Al-Futaisi, , Mol. Cryst. Liq. Cryst. 542, 123–131 (2011), Novel fluorinated ferroelectric organosiloxane liquid crystals.

[20] J. Naciri, C. Carboni, A. K. George; Liq. Cryst., 30, 219-225 (2003), Low transition temperature organosiloxane liquid crystals displaying a de Vries smectic A phase.

[21] J. Naciri, J. Ruth, G. Crawford, R. Shashidhar, B. R. Ratna; Chem. Mater., 7, 1397-1402 (1995), Novel ferroelectric and electroclinic organosiloxane liquid crystals.

[22] J. Dziaduszek, R. Dabrowski, K. Czuprynski, N. Bennis; Ferroelectrics., 343, 3–9 (2006), Ferroelectric Compounds with Strong Polar Cyano Group in Terminal Position.

[23] Z. Li, P. Salamon, A. Jakli, K. Wang, C. Qin, Q. Yang, C. Liu and J. Wen; Liq. Cryst., 37 427–433 (2010), Synthesis and mesomorphic properties of resorcyl di[4-(4-alkoxy-2,3-diflorophenyl)ethynyl] benzoate liquid crystals.

[24] Y. Yang, H. Li, J. Wen; Liq. Cryst., 34, 975-979 (2007), Synthesis and mesomorphic properties of chiral fluorinated liquid crystals.

[25] N. Shiratori, A. Yoshizawa, I. Nishiyama M. Fukumasa, A. Yokoyama, T. Hirai, M. Yamane; Mol. Cryst. Liq. Cryst. 199, 129-140 (1991), New Ferroelectric Liquid Crystals Having 2-Fluoro-2-Methyl Alkanoyloxy Group.

[26] A. Fafara, B. Gestblom, S. Wróbel, R. Dabrowski, W. Drzewiñski, D. Kilian, W. Haase; Ferroelectrics, 212, 79-90 (1998), Dielectric spectroscopy and electrooptic studies of new MHPOBC analogues.

[27] D. M. Potukuchi, A. K. George, C. Carboni, S. H. Alharthi, J. Naciri; Ferroelectrics, 300, 79-93 (2004), Low Frequency Dielectric Relaxation, Spontaneous Polarization, Optical Tilt Angle and Response Time Investigations in a Flourinated Ferroelectric Liquid Crystal, N125F2(R*).

[28] D. M. Potukuchi, A. K. George; Mol. Cryst. Liq. Cryst., 487, 92–109 (2008), Phase Transitions and Characterization in a Chiral Smectic-A $_{\text{de Vries}}$ Liquid Crystal by Low-Frequency Dielectric Spectroscopy.

[29] P. K. Mandal, S. Haldar, A. Lapanik, W. Haase; Jpn. J. Appl. Phys., 48, 011501-6 (2009), Induction and enhancement of ferroelectric smectic C* phase in multi-component room temperature mixtures.

[30] K. Hiraoka, A. Taguchi, Y. Ouchi, H. Takezoe and A. Fukuda; Jpn. J. Appl. Phys., 29, 1473-1476 (1990), Electric-Field-Induced Transitions among Antiferroelectric, Ferrielectric and Ferroelectric Phases in a Chiral Smectic MHPOBC.

[31] A. M. Biradar, S. Wróbel, and W. Haase; Phys. Rev. A, 39, 2693-2702 (1989), Dielectric relaxation in the smectic-A* and smectic-C* phases of a ferroelectric liquid crystal.

[32] T. Carlsson, B. Zeks, C. Filipic, A. Levstik; Phys. Rev. A, 42, 877–889 (1990), Theoretical model of the frequency and temperature dependence of the complex dielectric constant of ferroelectric liquid crystals near the smectic-C* - smectic-A phase transition.

[33] B. Zeks, M. Cepic, in Relaxation Phenomena: Liquid Crystals, Magnetic Systems, Polymers, High-TC Superconductors, Metallic Glasses; W. Haase, S. Wrobel, Eds. Springer Verlag: Berlin–Heidelberg, p 477 (2003).

[34] M. Buivydas, F. Gouda, S. T. Lagerwall, B. Stebler; Liq. Cryst., 18, 879–886 (1995), The molecular aspect of the double absorption peak in the dielectric spectrum of the antiferroelectric liquid crystal phase.

[35] Hyperchem 6.03, Hypercube Inc., Gainesville, FL, USA.

[36] S. Haldar, S. Barman, P. K. Mandal, W. Haase, R. Dabrowski; Mol. Cryst. Liq. Cryst., 528, 81-95 (2010), Influence of molecular core structure and chain length on the physical properties of nematogenic fluorobenzene derivatives.

[37] P. Sarkar, P. Mandal, S. Paul, R. Paul, R. Dabrowski, K. Czuprynski; Liq. Cryst., 30, 507-527 (2003), X-ray diffraction, optical birefringence, dielectric and phase transition properties of the long homologous series of nematogens 4-(trans-4′-n-alkylcyclohexyl) isothiocyanatobenzenes.

[38] D. Sinha, D. Goswami, P. K. Mandal, Ł. Szczucinski, R. Dabrowski; Mol. Cryst. Liq. Cryst. 562, 156-165 (2012), On the nature of molecular associations, static permittivity and dielectric relaxation in a uniaxial nematic liquid crystal.

[39] U. Manna, R. M. Richardson, A. Fukuda, J.K. Vij; Phys. Rev. E, 81, 050701–4 (2010), X-ray diffraction study of ferroelectric and antiferroelectric liquid crystal mixtures exhibiting de Vries SmA*-SmC* transitions.

[40] S. T. Lagerwall, Ferroelectric liquid crystals in : D. Demus, J. Goodby, G.W. Gray, H. W. Spiess, V. Vill (Eds.), Handbook of Liquid Crystals Vol. 2B – Low molecular weight liquid crystals, Wiley-Vch., Weinheim, pp 515-664 (1998).

[41] W. Piecek, Z. Raszewski, P. Perkowski, J. Przedmojski, J. Kedzierski, W. Drzewinski, R. Dabrowski, J. Zielinski; Ferroelectrics., 310, 125–129 (2004), Apparent tilt angle and structural investigations of the fluorinated antiferroelectric liquid crystal material for display application.

[42] J. P. F. Lagerwall, A. Saipa, F. Giesselmann, R. Dabrowski; Liq. Cryst. 31, 1175–1184 (2004), On the origin of high optical director tilt in a partially fluorinated orthoconic antiferroelectric liquid crystal mixture.

[43] K. D'havé, P. Rudquist, S.T. Lagerwall, H. Pauwels, W. Drzewiski, R. Dabrowski; Appl. Phys. Lett., 76, 3528-3530 (2000), Solution of the dark state problem in antiferroelectric liquid crystal displays.

[44] W. K. Robinson, C. Carboni, P. Kloess, S. P. Perkins, H. J. Coles; Liq. Cryst., 25, 301–307 (1998), Ferroelectric and antiferroelectric low molar mass organosiloxane liquid crystals.

[45] E. P. Haridas, S. S. Bawa, A. M. Biradar, S. Chandra, Jpn. J. Appl. Phys., 34, 3602-3606 (1995), Anisotropic surface anchoring conditions for gray-scale capability in high-tilt-angle ferroelectric liquid crystal.

[46] R. Blinc, B. Zeks; Phys. Rev. A. 18, 740-745 (1978), Dynamics of helicoidal ferroelectric smectic-C^* liquid crystals.

[47] T. Carlsson, B. Zeks, C. Filipic, A. Levstik; Physical Review A, 42, 877–889 (1990), Theoretical model of the frequency and temperature dependence of the complex dielectric constant of ferroelectric liquid crystals near the smectic-–smectic-A phase transition.

[48] N. A. Clark, S. T. Lagerwall, Introduction to ferroelectric liquid crystals, in: J.W. Goodby, R. Blinc, N. A. Clark, S. T. Lagerwall, M.A. Osipov, S.A. Pikin, T. Sakurai, K. Yoshino, B. Zeks (Eds), Ferroelectric Liquid Crystals Principles, Properties and Applications, Gordon and Breach, Philadelphia, 1991, pp. 1-97.

[49] D. Goswami, P. K. Mandal, R. Dabrowski; to be published.

[50] S. Sato, J. Hatano, S. Tatemori, H. Uehara, S. Saito, E. Okabe; Mol. Cryst. Liq. Cryst. A 328, 411-418 (1999), Antiferroelectricity of a Chiral Smectic Liquid Crystal Having Three Isolated Phenyl Rings in the Core.

[51] M. Marzec, W. Haase, E. Jakob, M. Pfeiffer, S. Wróbel; Liquid Crystals, 14, 1967- 1976 (1993), The existence of four dielectric modes in the planar oriented SmC* phase of a fluorinated substance.

[52] S. Wróbel, G. Cohen, D. Davidov, W. Haase, M. Marzec, M. Pfeiffer; Ferroelectrics, 166, 211–222 (1995), Dielectric, electro optic and X-ray studies of a room temperature ferroelectric mixture.

[53] J. M. Czerwiec, R. Dabrowski, K. Garbat, M. Marzec, M. Tykarska, A. Wawrzyniak, S. Wróbel; Liquid Crystals, 39, 1503–1511 (2012), Dielectric and electro-optic behaviour of two chiral compounds and their antiferroelectric mixtures.

[54] Y. P. Panarin, O. Kalinovskaya, J. K. Vij, and J. W. Goodby; Phys. Rev. E, 55, 4345-4353 (1997), Observation and investigation of the ferrielectric subphase with high qT parameter.

[55] Y. P. Panarin, O. Kalinovskaya, and J. K. Vij; Liq. Cryst., 25, 241-252 (1998), The investigation of the relaxation processes in antiferroelectric liquid crystals by broad band dielectric and electro-optic spectroscopy.

[56] J. K. Song, U. Manna, A. Fukuda and J. K. Vij; Appl. Phys. Lett., 93, 142903-3 (2008), Antiferroelectric dielectric relaxation processes and the interlayer interaction in antiferroelectric liquid crystals.

[57] U. Manna, J. K. Song, G. Power, and J. K. Vij; Phys. Rev. E, 78, 021711-8 (2008), Effect of cell surfaces on the stability of chiral smectic-C phases.

[58] U. Manna, J. K. Song, G. Power, J. K. Vij; Phys. Rev. E, 78, 021711-8 (2008), Effect of cell surfaces on the stability of chiral smectic-C phases.

[59] M. Buivydas, F. Gouda, G. Andersson, S. T. Lagerwall, B. Stembler, J. Bomelburg, G. Heppke, B. Gestblom; Liq. Cryst., 23, 723- 739 (1997), Collective and non-collective excitations

in antiferroelectric and ferrielectric liquid crystals studied by dielectric relaxation spectroscopy and electro-optic measurements.

[60] S. Haldar, K. C. Dey, D. Sinha, P. K. Mandal, W. Haase, P. Kula; Liq. Cryst., 39, 1196-1203 (2012), X-ray diffraction and dielectric spectroscopy studies on a partially fluorinated ferroelectric liquid crystal from the family of terphenyl esters.

[61] M. Marzec, A. Mikulko, S. Wrobel, R. Dabrowski, M. Darius and W. Haase; Liq. Cryst., 31, 153–159 (2004), Alpha sub-phase in a new ferroelectric fluorinated compound.

[62] P. Nayek, S. Ghosh, S. Roy, T. P. Majumder, R. Dabrowski; J. Mol. Liq. 175, 91–96 (2012), Electro-optic and dielectric investigations of a perfluorinated compound showing orthoconic antiferroelectric liquid crystal.

[63] P. Arora, A. Mikulko, F. Podgornov, W. Haase; Mol. Cryst. Liq. Cryst., 502, 1-8 (2009), Dielectric and electro-optic properties of new ferroelectric liquid crystalline mixture doped with carbon nanotubes.

[64] A. Mikulko, P. Arora, A. Glushchenko, A. Lapanik and W. Haase; Euro Phys. Lett., 87, 27009/1-4 (2009), Complementary studies of $BaTiO_3$ nanoparticles suspended in a ferroelectric liquid-crystalline mixture.

[65] P. K. Mandal, B. R. Jaishi, W. Haase, R. Dabrowski, M. Tykarska, P. Kula; Phase Transition, 79, 223–235 (2006), Optical microscopy, DSC and dielectric relaxation spectroscopy studies on a partially fluorinated ferroelectric liquid crystalline compound MHPO(13F)BC.

[66] W. N. Thurmes, M. D. Wand, R. T. Vohra, K. M. More; SPIE Conf. Proc. 3015, 1-7 (1997), FLC materials for microdisplay applications.

[67] M. Marzec, S. Wrobel, E. Gondek, R. Dabrowski; Mol. Cryst. Liq. Cryst., 410, 153–161 (2004), Room Temperature Antiferroelectric Phase Studied by Electrooptic Methods.

[68] F. Gouda, T. Carlsson, G. Andersson, S.T. Lagerwall, B. Stebler; Liq. Cryst., 16, 315-322 (1994), Manifestation of biquadratic coupling in the smectic C^* phase soft mode dielectric response.

[69] M. Marzec, S. Wröbel, S. Hiller, A. M. Biradar, R. Dabrowski, B. Gestblom, W. Haase; Mol. Cryst. Liq. Cryst., 302, 35-40 (1997), Dynamical properties of two ferroelectric phases of epoxy compound.

[70] R. Eidenschink, T. Geelhaar, G. Andersson, A. Dahlgren, K. Flatischler, F. Gouda, S. T. Lagerwall, K. Skarp; Ferroelectrics, 84, 167-181 (1988), Parameter characteristics of a ferroelectric liquid crystal with polarization sign reversal.

[71] A. K. Srivastavaa, R. Dhar, V. K. Agrawal, S. H. Lee, R. Dabrowski; Liq. Cryst., 35, 1101–1108 (2008), Switching and electrical properties of ferro- and antiferroelectric phases of MOPB(H)PBC.

[72] S. Essid, M. Manai, A. Gharbi, J. P. Marcerou, J. C. Rouillon; Liq. Cryst., 32, 307–313, (2005), Electro-optical switching properties for measuring the parameters of a ferroelectric liquid crystal.